



# Research on Active Firefighting Robot Navigation Based on the Improved AUKF Algorithm

Hubin Du, Qiuyu Li, Tanglong Chen, Yongtao Liu<sup>(✉)</sup>, Hengyuan Zhang, and Ziqian Guan

North  
China Institute of Science and Technology, Lang Fang, China  
lytliu@ncist.edu.cn

**Abstract.** It is difficult for autonomous mobile robots to rely on a single positioning method to obtain accurate pose information in complex indoor environments, so the real-time pose of the robot is generally obtained through multi-source fusion positioning during navigation. However, in the fusion localization algorithm based on AUKF (Adaptive Unscented Kalman Filtering), the Sage-Husa noise filter, which updates the white noise covariance of the random variable and the observed variable, is easy to cause the random variable system white noise covariance to lose non-negativity or the observed variable system to lose non-negativity. The white noise covariance loses its positive definiteness, which causes the divergence of the AUKF filtering algorithm and reduces the fusion accuracy. In order to solve the above problems, an improved AUKF algorithm is proposed that incorporates the covariance correction factor Roth, thereby improving the positive definiteness of the algorithm variance as well as the positioning accuracy of the fusion algorithm. Experimental results show that the improved AUKF algorithm achieves an average positioning accuracy of 95.23% in the x-axis direction, 94.06% in the y-axis direction, and 97.13% in the heading angle of the robot navigation coordinate system. It meets the requirements for accurate pose perception for autonomous mobile robot navigation in indoor environments.

**Keywords:** Autonomous Movement · Fusion Localization · Adaptive Unscented Kalman Filtering · Robot Navigation

## 1 Introduction

With the rapid development of China's economy and continuous urbanization, there is a growing need for autonomous mobile robot systems that are designed for mobile infrastructure management in cities, including electricity, communications, gas, water supply and drainage, etc. These systems are characterized by a variety of sensors, such as radar, ultrasound, laser, and image, to sense the surrounding environment and enable autonomous navigation [1, 2]. In recent years, the research on visual SLAM (Simultaneous Localization and Mapping) technology focuses on obtaining the visual features of

objects from the environment for localization [3, 4], Environmental memory [5, 6], 3D environment reconstruction [7], Semantic segmentation and environmental understanding [8, 9]. This research empowers the higher autonomy of robots. The current research hotspot is based on laser and visual SLAM technology for positioning methods. However, this method may result in significant errors or even navigation failure when there is a fire and a large amount of smoke in the room, making it unsuitable for active firefighting robots. The traditional track deduction technology based on an optical encoder has a cumulative error. Inertial Navigation System (INS) based on the inertial navigation measurement technology has noise interference, which affects positioning stability and accuracy. Ultra-Wideband (UWB) positioning technology is blocked and prone to Non-Line of Sight (NLOS) disturbances, which can cause large positioning instantaneous errors. These limitations inherent in a single-sensor positioning technology necessitate the adoption of a multi-sensor positioning information fusion method. This approach can effectively solve the disadvantages of single-sensor technology for indoor positioning, improve the accuracy of robot positioning, and increase the feasibility of accurate robot positioning in the presence of dense smoke.

The mainstream fusion positioning methods for robots include the Kalman Filter (KF) fusion positioning method, the Extended Kalman Filter (EKF) fusion positioning method, and the Untraced Kalman Filter (UKF) fusion positioning method [10]. KF [11] uses the linear system state equation to optimally estimate the current state of the system through input and output measurement data. However, traditional KF algorithms can only be applied to linear systems. With the proposal of EKF [12], the application of traditional KF has been extended to nonlinear systems. EKF is a first-order Taylor series expansion of a nonlinear system in which the higher-order term is ignored during the linearization of its first derivative, thereby transforming it into a linear problem. However, EKF also has two problems: linearization error and calculation of the more complex Jacobian matrix. To address these issues, based on UKF, Arasaratnam et al. [13] proposed the Cubature Kalman filter (CKF), which is based on numerical integration. It can outperform EKF and UKF when handling nonlinear states and measurement equations and give better nonlinear approximation performance and stability. Moreover, CKF is a simpler and faster alternative to particle filtering.

In order to improve the positioning accuracy of firefighting robots in indoor environments, this paper proposes a method based on track deduction, IMU and UWB system measurement data.

## **2 Multi-source Fusion Localization Method Based on Improved AUKF Algorithm**

The localization data obtained in the absence of Adaptive Unscented Kalman Filtering (AUKF) exhibits nonlinear characteristics. In practical test environments, non-Gaussian data distribution can almost fit a Gaussian distribution. The existing data indicate that the pose 1 information obtained by encoder track deduction contains cumulative errors, while the pose 2 information obtained by INS and gyroscope equipment contains instantaneous

errors with relatively small cumulative errors. Since the error of pose 1 information approximately follows the Gaussian distribution, the AUKF algorithm [14] can optimize the information collected by pose 1 and pose 2, thereby reducing cumulative and instantaneous errors. Filtering can be employed to obtain a more accurate estimated position, ultimately enabling high-precision positioning for robots in indoor environments.

When fusing the AUKF algorithm, the pose 1 information obtained by the gyroscope at time  $t$  is first set to  $U(t)T = U(t)T = (x_e, y_e, \theta_e)$ , the predicted quantity. The difference between the current location information and the previous location information is set to  $\Delta U(t)T$ . The status information pose 2 obtained from the UWB + IMU at time  $t$  is denoted by  $Z(t)T = (x_u, y_u, \theta_u)$  as an observational measure. The error of pose 1 and pose 2 is set to  $W(m)$  and  $V(m)$ , and the noise variances are set to  $Q$  and  $R$ , respectively. The predicted error of the estimated position (fusion position) information  $X(m)$  in each  $n \times \Delta t$  time is  $P$ . Among the above parameters,  $U(t)$ ,  $Z(t)$ ,  $W(t)$ ,  $V(t)$ ,  $Q$ ,  $R$ , and  $P$  are all three-dimensional matrices, and  $Kg_{(t)}$  is the gain matrix of the filter. In the AUKF algorithm positioning information fusion, the state values of pose 1 and pose 2 are used as the predictor array and the observed data, respectively. To implement the AUKF algorithm, the following steps should be carried out:

Step 1: Initialization

$$\hat{x}_0 = E[X_0] \quad (1)$$

$$P_0 = E[(x_0 - \hat{x}_0)(x_0 - \hat{x}_0)^T] \quad (2)$$

where  $\hat{x}_0$  is the expected mean of the initial state  $\mathbf{x}_0$ , and  $P_0$  is the expected covariance matrix of the initial state estimation error.

Step 2: Calculate the Sigma Points

$$X_{k-1} = [\hat{x}_{k-1} \quad \hat{x}_{k-1} \pm \sqrt{(n + \lambda)P_{k-1}}] \quad (3)$$

The sigma point set  $X(k-1)$  can be defined as follows:

$$\begin{cases} X_{0,k-1} = \hat{x}_{k-1} \\ X_{i,k-1} = \hat{x}_{k-1} + (\sqrt{(n + \lambda)P_{k-1}})_i, & i = 1, 2, \dots, n \\ X_{i,k-1} = \hat{x}_{k-1} - (\sqrt{(n + \lambda)P_{k-1}})_{i-n}, & i = n + 1, \dots, 2n \end{cases} \quad (4)$$

where the composite scaling parameter  $\lambda$  is defined as  $\lambda = \alpha^2(n + \kappa) - n$ . The 3-dimensional array is considered as the state vector, so  $n$ , the dimension of the state vector, is set to 3.  $\alpha$  represents a positive parameter that controls the spread of the sigma point and is set to 1.  $\kappa$  as the secondary scaling parameter is set to  $3 - n = 0$ .

Step 3. Status step prediction

$$X_{k|k-1} = f(X_{k-1}) \quad (5)$$

$$\hat{x}_{k|k-1} = \sum_{i=0}^{2n} W_i^{(m)} X_{i,k|k-1} \quad (6)$$

$$P_{k|k-1} = \sum_{i=0}^{2n} W_i^{(c)} [X_{i,k|k-1} - \hat{x}_{k|k-1}] [X_{i,k|k-1} - \hat{x}_{k|k-1}]^T + Q_k \quad (7)$$

Here,  $X_{k|k-1}$  refers to the linear state vector of the state transfer function at  $k$ ,  $W_i^{(m)}$  the average weight, and  $W_i^{(c)}$  the covariance weight. So, the piecewise expression is defined as follows:

$$\begin{cases} W_0^{(m)} = \frac{\lambda}{n+\lambda} \\ W_0^{(c)} = \frac{\lambda}{n+\lambda} + (1 - \alpha^2 + \beta) \\ W_i^{(m)} = W_i^{(c)} = \frac{1}{2(n+\lambda)} \end{cases}, i = 1, 2, \dots, 2n \quad (8)$$

where  $\beta$  is a non-negative parameter that combines partial prior distribution data. In this article,  $\beta$  is generally set to 2, which is optimal for a normal distribution

Step 4. Status update remediation

$$Z_{k|k-1} = h(X_{k|k-1}) \quad (9)$$

$$\hat{z}_{k|k-1} = \sum_{i=0}^{2n} W_i^{(m)} Z_{i,k|k-1} \quad (10)$$

where  $\hat{z}_{k|k-1}$  is the measurement vector of the function at  $k$ ;

$$P_{zz,k|k-1} = \sum_{i=0}^{2n} W_i^{(c)} [Z_{i,k|k-1} - \hat{z}_{k|k-1}] [Z_{i,k|k-1} - \hat{z}_{k|k-1}]^T + (R + Roth) \quad (11)$$

$$P_{xz,k|k-1} = \sum_{i=0}^{2n} W_i^{(c)} [X_{i,k|k-1} - \hat{x}_{k|k-1}] * [Z_{i,k|k-1} - \hat{z}_{k|k-1}]^T \quad (12)$$

where  $P_{zz,k|k-1}$  is the expected measurement error covariance matrix, and  $P_{xz,k|k-1}$  is the expected measurement error mutual variance matrix. In traditional AUKF, the Sage-Husa noise filter updates the white noise covariance of random variables and observation variable systems. However, if the absolute value of the non-zero element in the derivation exceeds a specific threshold or the self-covariance element is negative, the white noise covariance of the random variable system can lose non-negativity or that of the observation variable system can lose positive certainty. These issues can cause the AUKF filter to diverge and result in decreased accuracy [15]. In order to overcome the above problems, this paper introduces the difference between the observed estimated mean and the predicted estimated mean as a follow-up correction coefficient into the measurement error covariance matrix. This approach helps prevent the white noise covariance from becoming indeterminate and improve the accuracy of the algorithm fitting [16].

In Eq. (11),  $Roth$  represents the difference between the estimated mean of the observation and the prediction, which is computed as  $Roth = (Z_{pred} - X_{pred})R$ . This parameter affects UKF gain  $K_k$  to achieve process update adaptation [17, 18].

$$K_k = P_{xz,k|k-1} P_{zz,k|k-1}^{-1} \quad (13)$$

$$\hat{x}_k = \hat{x}_{k|k-1} + K_k(z_k - \hat{z}_{k|k-1}) \quad (14)$$

$$P_k = P_{k|k-1} - K_k P_{xz,k|k-1} K_k^T \quad (15)$$

where  $K_k$  is the filter gain,  $\hat{x}_k$  the filter estimate and  $P_k$  the filter error. It demonstrates that when there is a random error or abnormal jitter of the robot at  $k-1$ , the state vector estimation  $\hat{x}_{k|k-1}$  will also have a corresponding error, which will be corrected by the covariance correction factor Roth [19].

$P_{(t-1)}$  is the one-step prediction estimation bias covariance matrix, and  $P_{(t|m-1)}$  is the measurement correction estimation bias covariance matrix. The initial value of  $P$  is set to  $[1 \ 1 \ 1]$ , and non-zero values are sufficient. The initial values of noise variance  $Q$  and  $R$  are experimentally determined with effective values of  $Q = [0.001, 1, 1]$  and  $R = [200, 200, 1]$ . This decreases the error caused by nonlinear positioning value and increases the efficiency of the algorithm [20, 21].

The filtering and fusion process outlined above is effective in reducing the impact of other types of noise on both the accumulated error and the instantaneous error [22]. In summary, the improved AUKF algorithm proposed in this paper can allow the firefighting robot to obtain stable and high-precision position information during its navigation.

### 3 Experimental Analysis

Because the AUKF algorithm is prone to lose positive certainty, the filtering effect of the algorithm diverges and the accuracy decreases [23]. In order to overcome the above problems, the Roth function is introduced into the measurement error covariance matrix in this model. This method can mitigate the problem that the covariance cannot be positively determined and meanwhile it improves the accuracy of the algorithm fitting [24]. In order to verify the effectiveness of the improved algorithm, the active firefighting robot starts from the navigation system coordinate point (120,720) and moves along a rectangular path of 320\*480 cm. The navigation trajectory of the tested robot is depicted in Fig. 1.

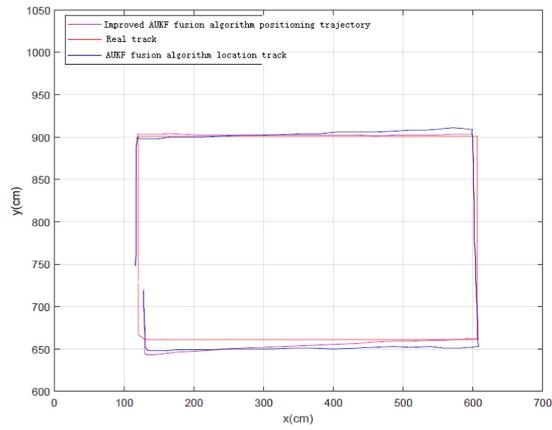
In Fig. 1(b), the red trajectory represents the real motion trajectory of the active firefighting robot, the blue one the trajectory based on the traditional AUKF algorithm, and the pink one the trajectory based on the improved AUKF algorithm. Figure 1 demonstrates that the fusion effect of the improved algorithm is closer to that of the real trajectory, with a smaller average error.

During the navigation of autonomous mobile robots, it is crucial to accurately determine the robot's current heading angle in addition to its real-time navigation coordinate position. In this way, accurate control over the autonomous movement of robots can be realized [25, 26].

This paper investigated the AUKF positioning fusion algorithm and the improved AUKF positioning fusion algorithm based on the performance test of the trajectory-deduced pose and UWB + IMU pose obtained by a robot moving in a rectangular motion in a laboratory setting. The test data corresponding to Fig. 2 is shown in Table 1. In Fig. 2, subfigures (a), (b), and (c) demonstrate the classical AUKF algorithm based



(a) The operating trajectory environment of the robot

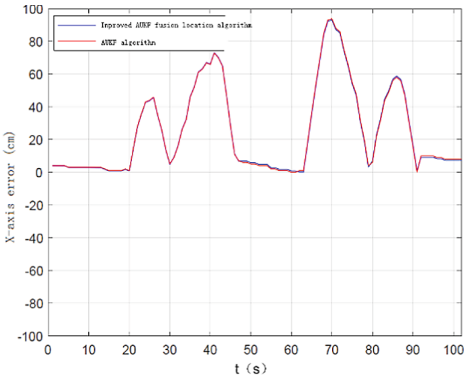


(b) Robot rectangular motion navigation trajectory

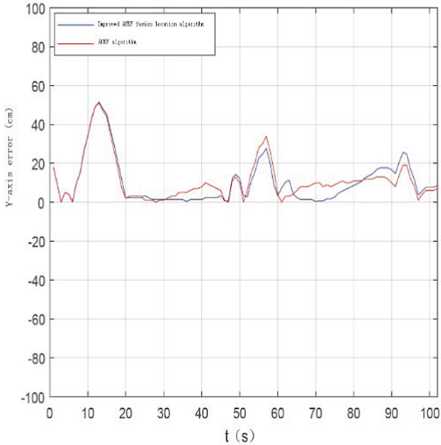
**Fig. 1.** Actual test environment and navigation trajectory of robot

on the compact combination navigation model and the improved AUKF algorithm in the x-axis, y-axis, and heading angle error curves, respectively.

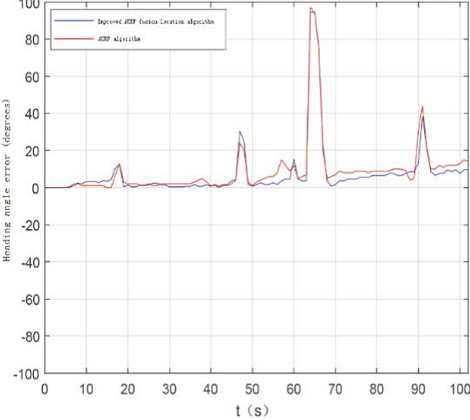
As shown in Table 1, the improved AUKF algorithm outperforms the traditional AUKF in three aspects: absolute error of the x-axis, absolute error of the y-axis, and absolute error of heading angle [27, 28]. Therefore, the fusion positioning based on the improved AUKF algorithm in this paper can meet requirements for long-distance and long-term navigation positioning of active firefighting robots. Furthermore, the introduction of a heading angle is the prerequisite for the subsequent path planning of the robot.



(a) Improve the x-axis error of the AUKF algorithm and the AUKF algorithm



(b) Improve the y-axis error of AUKF algorithm and AUKF algorithm



(c) Improve the heading angle error of the AUKF algorithm and the AUKF algorithm

**Fig. 2.** Error Analysis of Navigation Position and Attitude Based on Improved AUKF Algorithm

**Table 1.** Comparison of absolute positioning error between AUKF algorithm and improved AUKF algorithm

type	AUKF fusion location algorithm	This paper improves the AUKF fusion location algorithm
Absolute error of y-axis (cm)x	25.2304	25.0896
Absolute error of y-axis (cm)	11.2623	10.487
Absolute average error of heading angle (degrees)	9.14216	7.53287

## 4 Conclusion

- (1) In this paper, the AUKF algorithm is improved by incorporating the covariance correction factor Roth, which ensures the positivity of the white noise covariance in the algorithm and improves the accuracy of the algorithm for positioning.
- (2) Experimental results demonstrate that the multi-source fusion positioning algorithm based on the improved AUKF algorithm can enhance the accuracy of the X and Y axes and the heading angle of the indoor autonomous mobile robot in the navigation coordinate system, which meets the requirements of rapid navigation for the robot.

**Acknowledgments.** S&T Program of Hebei (22375411D).

## References

1. Gao Wei, Hou Congyi, Xu Wanyang, etc Research progress and prospect of indoor navigation and positioning technology [J] Journal of Navigation and Positioning, 2019, 7 (1): 10–17
2. Dai Rui Obstacle-avoidance information perception and behavior uncertainty processing of storage robot in unstructured environment [D] University of Electronic Science and Technology, 2019.
3. Wu Junjun. Research on key algorithms for simultaneous positioning and map construction of mobile robot vision [D] South China University of Technology, 2013
4. Luwei Research on key technologies of high-precision real-time visual positioning [D] Zhejiang University, 2015.
5. Li Bo. Research on visual closed-loop detection of mobile robot based on scene appearance modeling [D] Chongqing University, 2011
6. Liang Zhiwei, Chen Yanyan, Zhu Songhao, etc. Closed-loop detection algorithm for monocular vision based on visual dictionary [J] Pattern Recognition and Artificial Intelligence, 2013, 26 (6): 561–570
7. Mei Feng, Liu Jing, Li Chunpeng, etc Indoor scene reconstruction based on RGB - D depth camera [J] Chinese Journal of Image Graphics, 2015, 20 (10): 1366–1373.



8. Bao S Y, Bagra M, Chao Y W, et al. Semantic structure from motion with points, regions, and objects[C]// Conference on Computer Vision and Pattern Recognition. IEEE, 2012:2703–2710.
9. Hane C, Zach C, Cohen A, et al. Joint 3D scene reconstruction and class segmentation[C]// Conference on Computer Vision and Pattern Recognition. IEEE, 2013:97–104.
10. Wu Xian. Research on mobile robot positioning method based on multi-sensor information fusion [D]. Beijing Jiaotong University, 2016.
11. Kalman R E, Bucy R S. New results in linear filtering and prediction theory[J]. Transactions of the Asme-Journal of Basic Engineering, 1961, 83(83):95-107.
12. Ljung L. Asymptotic behavior of the extended Kalman filter as a parameter estimator for linear systems[J]. Automatic Control IEEE Transactions on, 2003, 24 (1):36 -50.
13. Arasaratnam I, Haykin S. Cubature Kalman filters[J]. IEEE Transactions on Automatic Control, 2009, 54 (6):1254-1269.
14. Zhang Bin, Wang Y-x, Shao X, et al. Precise Robot Indoor Localization Based on Information Fusion of Heterogeneous Sensors[J]. Control Engineering of China, 2018, 25(7):1335–1343.
15. Fang X, Nan L, Jiang Z , et al. Robust node position estimation algorithms for wireless sensor networks based on improved adaptive Kalman filters[J]. Computer Communications, 2017(11):69-81.
16. Bing Hua, Zhiwen Zhang, Yunhua Wu, Zhiming Chen. Autonomous navigation algorithm based on AUKF filter about fusion of geomagnetic and sunlight directions[J]. International Journal of Intelligent Computing and Cybernetics, 2018, 11(4).
17. Claudio Urrea, Rodrigo Muñoz. Joints Position Estimation of a Redundant Scara Robot by Means of the Unscented Kalman Filter and Inertial Sensors[J]. Asian Journal of Control, 2016, 18(2).
18. Xiang Guofei, Dian Songyi, Zhao Ning, Wang Guodong. Semantic-Structure-Aware Multi-Level Information Fusion for Robust Global Orientation Optimization of Autonomous Mobile Robots[J]. Sensors, 2023, 23(3).
19. Xiang Guofei , Dian Songyi, Zhao Ning, Wang Guodong. Semantic-Structure-Aware Multi-Level Information Fusion for Robust Global Orientation Optimization of Autonomous Mobile Robots[J]. Sensors, 2023, 23(3).
20. Talaat Fatma M., Ibrahim Abdelhameed, ElKenawy ElSayed M., Abdelhamid Abdelaziz A., Alhussan Amel Ali, Khafaga Doaa Sami, Salem Dina Ahmed. Route Planning for Autonomous Mobile Robots Using a Reinforcement Learning Algorithm[J]. Actuators, 2022, 12(1).
21. Rafai Anis Naema Atiyah, Adzhar Noraziah, Jaini Nor Izzati. A Review on Path Planning and Obstacle Avoidance Algorithms for Autonomous Mobile Robots[J]. Journal of Robotics, 2022, 2022.
22. SUN Ming, CHEN Rihui, CHEN Yan , CHEN Xiaoice. Improvement of hybrid navigation algorithm of autonomous mobile robot(AMR)[J]. Modern Information Technology, 2022, 6(15):139–147.) DOI:<https://doi.org/10.19850/j.cnki.2096-4706.2022.15.037>.
23. ZHANG Yimin, HAN Haimin, WANG Liyu. Motion control and coordination problems and optimization of autonomous mobile robots [J]. New Industrialization, 2022, 12(06):241–245.) DOI: <https://doi.org/10.19335/j.cnki.2095-6649.2022.6.057>.
24. WANG Bin. Research on path planning of indoor omnidirectional autonomous mobile robot [D]. Zhongyuan University of Technology, 2022. DOI:<https://doi.org/10.27774/d.cnki.gzygx.2022.000164>.
25. Shi Cun, Wang Ying, Che Yuqiu. Motion control and coordination of autonomous mobile robot [J]. Decision Exploration(middle), 2020(12):57–58.
26. SHAO Mingzhi, HE Tao, ZHU Yongping, CHEN Wenzhong. Research on navigation and positioning of mobile robot based on multi-sensor information fusion[J]. Machine Tool and Hydraulics, 2023, 51(05):8–13.)

27. Long Yingkai, Du Mingming, Luo Xiaoxiao, Li Siqian, Jiang Xiping. Improved VMD-+ACO Algorithm Navigation and Positioning Technology for Robot Electric Power Inspection[J]. International Transactions on Electrical Energy Systems, 2022, 2022.
28. Wang Ziyu, Hu Bin. Research on navigation and control technology of fire robot[J]. Fire Science and Technology, 2022, 41(09): 1263–1267.

**Open Access** This chapter is licensed under the terms of the Creative Commons Attribution-NonCommercial 4.0 International License (<http://creativecommons.org/licenses/by-nc/4.0/>), which permits any noncommercial use, sharing, adaptation, distribution and reproduction in any medium or format, as long as you give appropriate credit to the original author(s) and the source, provide a link to the Creative Commons license and indicate if changes were made.

The images or other third party material in this chapter are included in the chapter's Creative Commons license, unless indicated otherwise in a credit line to the material. If material is not included in the chapter's Creative Commons license and your intended use is not permitted by statutory regulation or exceeds the permitted use, you will need to obtain permission directly from the copyright holder.

